Journal of Medicinal Chemistry

Article

C-Labeling of *N*-[4-[4-(2,3-Dichlorophenyl)piperazin-1-yl]butyl]arylcarboxamide Derivatives and Evaluation as Potential Radioligands for PET Imaging of Dopamine D Receptors

Elia A. Turolla, Mario Matarrese, Sara Belloli, Rosa M. Moresco, Pasquale Simonelli, Sergio Todde, Ferruccio Fazio, Fulvio Magni, Marzia Galli Kienle, Marcello Leopoldo, Francesco Berardi, Nicola A. Colabufo, Enza Lacivita, and Roberto Perrone

J. Med. Chem., **2005**, 48 (22), 7018-7023• DOI: 10.1021/jm050171k • Publication Date (Web): 30 September 2005

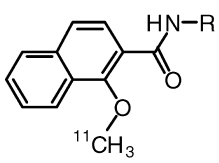

[^{11}C]**1**

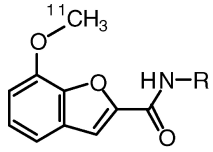

[^{11}C]**2**

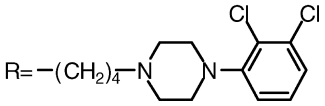

More About This Article

Additional resources and features associated with this article are available within the HTML version:

- Supporting Information
- Links to the 3 articles that cite this article, as of the time of this article download
- Access to high resolution figures
- Links to articles and content related to this article
- Copyright permission to reproduce figures and/or text from this article

View the Full Text HTML

^{11}C-Labeling of *N*-[4-[4-(2,3-Dichlorophenyl)piperazin-1-yl]butyl]arylcarboxamide Derivatives and Evaluation as Potential Radioligands for PET Imaging of Dopamine D_3 Receptors

Elia A. Turolla,[†] Mario Matarrese,[†] Sara Belloli,[†] Rosa M. Moresco,[†] Pasquale Simonelli,[†] Sergio Todde,[†] Ferruccio Fazio,*[,†] Fulvio Magni,[‡] Marzia Galli Kienle,[‡] Marcello Leopoldo,[§] Francesco Berardi,[§] Nicola A. Colabufo,[§] Enza Lacivita,[§] and Roberto Perrone[§]

Institute of Molecular Bioimaging and Physiology-CNR, University of Milano/Bicocca, Institute San Raffaele, Via Olgettina 60, 20132 Milano, Italy, DIMESAB, University of Milano/Bicocca, via Cadore 48, 20052 Monza (MI), Italy, and Dipartimento Farmaco-Chimico, Università degli Studi di Bari, via Orabona 4, 70125 Bari, Italy

Received February 22, 2005

The selective dopamine D_3 receptor ligands *N*-4-[4-[(2,3-dichlorophenyl)piperazin-1-yl]butyl]1-methoxy-2-naphthalencarboxamide (**1**) and *N*-4-[4-[(2,3-dichlorophenyl)piperazin-1-yl]butyl]-7-methoxy-2-benzofurancarboxamide (**2**) were labeled with ^{11}C ($t_{1/2}$ = 20.4 min) as potential radioligands for the noninvasive assessment of the dopamine D_3 neurotransmission system in vivo with positron emission tomography (PET). The radiosynthesis consisted in an O-methylation of the *des*-methyl precursors *N*-[4-[4-(2,3-dichlorophenyl)piperazin-1-yl]butyl]-1-hydroxy-2-naphthalenecarboxamide (**3**) and *N*-[4-[4-(2,3-dichlorophenyl)piperazin-1-yl]butyl]-7-hydroxy-2-benzofurancarboxamide (**4**) with [^{11}C]methyl iodide using *t*BuOK/HMPA and KOH/DMSO, respectively. The radiotracers [^{11}C]**1** and [^{11}C]**2** were obtained in 35 min with over 99% radiochemical purity, 74 ± 37 GBq/μmol of specific radioactivity, 13% and 26% radiochemical yield (EOB, decay-corrected). Distribution studies in rats demonstrated that the new tracers [^{11}C]**1** and [^{11}C]**2** cross the blood−brain barrier and localize in the brain. However, the kinetics of cerebral uptake did not reflect the regional expression of the D_3 receptors. Despite their in vitro pharmacological profile, [^{11}C]**1** and [^{11}C]**2** do not display an in vivo behavior suitable to image D_3 receptor expression using PET.

Introduction

Dopamine interacts with a family of different receptor subtypes. Currently, five dopamine receptor subtypes have been characterized. These subtypes include D_1−D_5 receptors, which are grouped into the D_1-like family (D_1 and D_5) and the D_2-like family (D_2, D_3, and D_4). This classification is based upon similarities in primary structure and pharmacological properties.[1]

Despite structural and pharmacological similarities between D_2 and D_3 dopamine receptor subtypes, there are some fundamental differences: (a) neuroanatomical expression; (b) efficiency and diversity of coupling to G proteins; (c) receptor regulation following pharmacological intervention.

The distribution of the dopamine D_3 receptor in the CNS has received attention because of its specific distribution in limbic areas and its low expression in the striatum. This distribution is interesting because those neuroleptics showing preference for D_3 receptor seem to be less prone to induce extrapyramidal side effects such as tardive dyskinesia,[2] so D_3 receptor could be a target for new antipsychotics. The D_3 receptor subtype could also be involved in Parkinson's disease, and it could play a modulatory role in the self-administration of psychostimulant drugs.

For these reasons, there is a need for radiotracers to study the dopamine D_3 receptors with positron emission tomography (PET), and to our knowledge, radioligands with high D_3 selectivity are not available. In fact, PET studies have been performed by using D_2/D_3 radiotracers such as [^{11}C]raclopride (**5**)[3] or [^{11}C]fallypride (**6**).[4] However, some proposed selective agents such as [^{11}C]GR-218231 (**7**)[5] (pK_i = 9.0 nM) and 5-bromo-*N*-(4-(4-(2,3-dichlorophenyl)piperazin-1-yl)butyl)-2-[^{11}C]methoxy-3-methoxybenzamide (**8**)[6] (K_i = 2 nM) have been prepared, and validation studies in rats are in progress. In addition, the highly selective dopamine D_3 agent RGH-1756 (**9**), which showed promising binding characteristics for D_3 receptor in vitro, has been radiolabeled with carbon-11 ($t_{1/2}$ = 20.4 min, β^+ = 99.8%) and characterized in the cynomolgus monkey brain[7] (Chart 1).

Recently, a new series of *N*-[4-[4-(2,3-dichlorophenyl)-piperazin-1-yl]butyl]arylcarboxamide derivatives displaying subnanomolar affinity and high specificity for the dopamine D_3 receptors have been reported.[8] Among them, *N*-4-[4-[(2,3-dichlorophenyl)piperazin-1-yl]butyl]1-methoxy-2-naphthalencarboxamide (**1**) and *N*-4-[4-[(2,3-dichlorophenyl)piperazin-1-yl]butyl]-7-methoxy-2-benzofurancarboxamide (**2**) were selected for their binding profile and labeled in the *O*-methyl position with the positron emitter ^{11}C to obtain potential dopamine D_3 radioligands for PET studies (Table 1).

* To whom correspondence should be addressed. Phone: +39-02-26432716. Fax: +39-02-26415202. E-mail: fazio.ferruccio@hsr.it.
† Institute of Molecular Bioimaging and Physiology-CNR; University of Milano/Bicocca.
‡ DIMESAB, University of Milano/Bicocca.
§ Dipartimento Farmaco-Chimico, Università degli Studi di Bari.

10.1021/jm050171k CCC: $30.25
Published on Web 09/30/2005

Chart 1

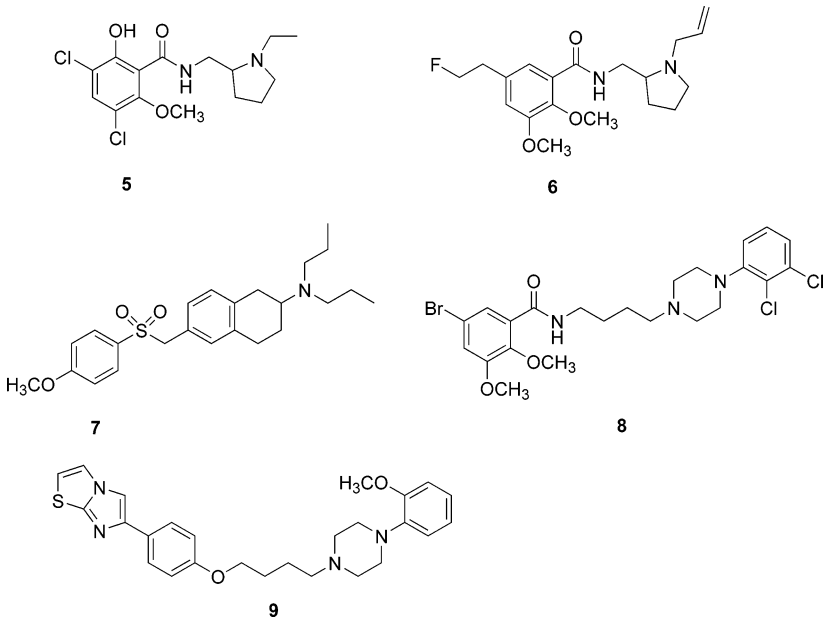

Table 1. Binding Profile and Lipophilicity Properties of Derivatives **1** and **2**

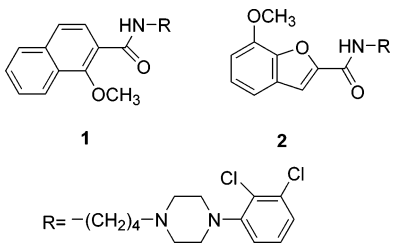

	K_i, nM[a]							
compd	D_3	D_2	D_4	5-HT_{1A}	α_1	σ_1	σ_2	CLogP
1	0.60	720	830	575	5100	342	164	5.61
2	0.13	720	373	184	110	180	342	4.98

[a] Data taken from ref 8.

In this report, we describe the ^{11}C radiolabeling of **1** and **2** by O-methylation of the corresponding *des*-methyl precursors *N*-[4-[4-(2,3-dichlorophenyl)piperazin-1-yl]-butyl]-1-hydroxy-2-naphthalenecarboxamide (**3**) and *N*-[4-[4-(2,3-dichlorophenyl)piperazin-1-yl]butyl]-7-hydroxy-2-benzofurancarboxamide (**4**) with [^{11}C]methyl iodide, the results of biodistribution, and the autoradiographic studies performed in rats to evaluate their potential use as PET radioligands.

Results

Chemistry. Derivatives [^{11}C]**1** and [^{11}C]**2** were successfully prepared by O-[^{11}C]methylation of the corresponding phenolic precursors **3** and **4** with [^{11}C]methyl iodide using potassium-*tert*-butoxide and potassium hydroxide, respectively. The key intermediates **3** and **4** were synthesized by demethylation with sodium thioethoxide[9] of the corresponding methoxyderivatives **1** and **2** (Scheme 1).[8]

Radiochemistry. As shown in Tables 2 and 3, first, sodium and potassium hydroxide in DMSO were employed for deprotonation of **3** and **4**. Using 5 M KOH in DMSO, we obtained [^{11}C]**2** in a yield of 59% with little development of ^{11}C-methanol and other ^{11}C-impurities.

Scheme 1[a]

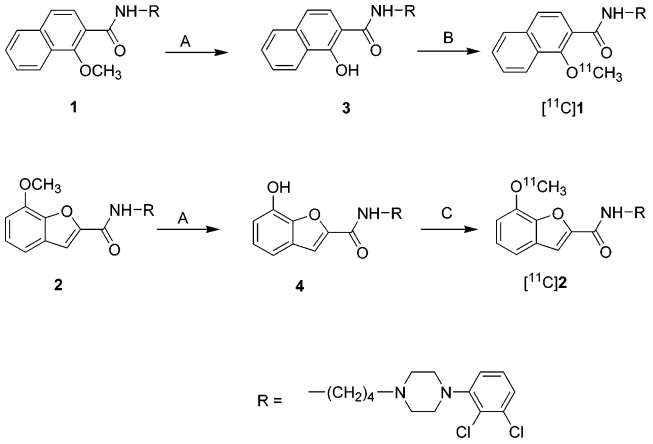

[a] Reagents: (A) C_2H_5SNa; (B) *t*BuOK, [^{11}C]CH_3I; (C) 5 M KOH, [^{11}C]CH_3I.

When other bases were used, the final yield was lower (Table 3). The use of an aqueous solution base in DMSO for [^{11}C]**1** was less effective, giving a very low reaction yield. Using a different reaction solvent (i.e., HMPA) with 1 M KOH, we still obtain a low yield, due to the expected formation of hydrolyzed byproducts. The best result for this tracer was, rather, obtained with a bulky base such as *t*BuOK under nonaqueous conditions (Table 2).

The overall decay-corrected radiochemical yield of the [^{11}C]O-methylation was 13% for [^{11}C]**1** and 26% for [^{11}C]-**2**. At the end of synthesis (EOS), the specific radioactivity was 74 ± 37 GBq/μmol. The average time of radiosynthesis was 35 min, including radioligand formulation for intravenous administration. In a typical experiment, starting from 30 GBq of [^{11}C]CO_2, 1.1 GBq of [^{11}C]**1** and 2.2 GBq of [^{11}C]**2** were obtained with a chemical purity of 99% and a radiochemical purity of 100%.

Identification of the final radioactive radioligands was confirmed by co-injection of the authentic sample of **1** or **2** on RP-HPLC and by mass spectrometry analysis of the carrier-added radiosynthesis products.

Table 2. Radiolabeling of **1** with [^{11}C]Methyl Iodide[a]

compd	solvent	base	amount (μmol)	T, °C	[^{11}C]**1** (%)	other [^{11}C] impurities (%)	[^{11}C]CH_3OH (%)	n
3	DMSO	5 M KOH	10	80/115	0	100		3
3	DMSO	5 M NaOH	10	80	17 ± 1	67 ± 6	16 ± 5	3
3	DMSO	10 M NaOH	25	100	18 ± 2	63 ± 5	19 ± 5	3
3	HMPA	1 M KOH	10	80	19 ± 3	80 ± 2		3
3	HMPA	*t*BuOK	12.5	80/100	24 ± 7	61 ± 6	17 ± 3	3

[a] Time for all methylations is 5 min for 1 mg of **3**. Data points represent the mean ± SD.

Table 3. Radiolabeling of **2** with [^{11}C]Methyl Iodide[a]

compd	solvent	base	amount (μmol)	T, °C	[^{11}C]**2** (%)	other [^{11}C] impurities (%)	[^{11}C]CH_3OH (%)	n
4	DMSO	1 M TBAOH	2.3	80/100	40 ± 4	53 ± 2	8 ± 1	3
4	DMSO	1 M KOH	3	80	36 ± 8	50 ± 2	4 ± 4	3
4	DMSO	5 M KOH	10	80	59 ± 10	31 ± 5	10 ± 6	12

[a] Time for all methylations is 5 min for 1 mg of **4**. Data points represent the mean ± SD.

Table 4. Regional Brain Distribution of [^{11}C]**1** in Rats[a]

tissue	5 min	15 min	30 min	60 min
blood	0.066 ± 0.011	0.060 ± 0.088	0.057 ± 0.012	0.074 ± 0.002
plasma	0.083 ± 0.001	0.074 ± 0.008	0.082 ± 0.005	0.088 ± 0.001
prefrontal cortex	0.089 ± 0.042	0.090 ± 0.006	0.101 ± 0.028	0.109 ± 0.008
nucleus accumbens	0.087 ± 0.059	0.104 ± 0.000	0.101 ± 0.015	0.090 ± 0.021
anterior striatum	0.074 ± 0.045	0.069 ± 0.017	0.081± 0.001	0.099 ± 0.004
central striatum	0.085 ± 0.027	0.077 ± 0.006	0.086 ± 0.014	0.095 ± 0.014
posterior striatum	0.070 ± 0.030	0.090 ± 0.010	0.087 ± 0.022	0.087 ± 0.014
cerebellum	0.092 ± 0.024	0.088 ± 0.011	0.087 ± 0.020	0.098 ± 0.016

[a] Radioactivity concentration is expressed as % of injected dose per gram of tissue (%ID/g). Values are expressed as mean ± SD of three rats for each time point.

Table 5. Regional Brain Distribution of [^{11}C]**2** in Rats[a]

tissue	5 min	15 min	30 min	60 min
blood	0.074 ± 0.026	0.051 ± 0.000	0.030 ± 0.005	0.030 ± 0.005
plasma	0.079 ± 0.019	0.058 ± 0.008	0.030 ± 0.003	0.033 ± 0.002
prefrontal cortex	0.088 ± 0.032	0.054 ± 0.019	0.060 ± 0.007	0.067 ± 0.004
nucleus accumbens	0.077 ± 0.031	0.049 ± 0.017	0.062 ± 0.014	0.071 ± 0.019
anterior striatum	0.072 ± 0.031	0.043 ± 0.011	0.050 ± 0.009	0.050 ± 0.006
central striatum	0.069 ± 0.025	0.049 ± 0.02	0.053 ± 0.007	0.058 ± 0.004
posterior striatum	0.053 ± 0.012	0.044 ± 0.025	0.051 ± 0.012	0.067 ± 0.017
cerebellum	0.078 ± 0.025	0.050 ± 0.020	0.056 ± 0.016	0.051 ± 0.003

[a] Radioactivity concentration is expressed as % of injected dose per gram of tissue (%ID/g).

Biological Evaluation. Cerebral Distribution of [^{11}C]1 and [^{11}C]2 in Rat Brain. The regional distribution of the two radiotracers [^{11}C]**1** and [^{11}C]**2** in the rat brain are reported in Tables 4 and 5. Values are expressed as mean ± SD of three rats for each time point.

Although Levant has found high concentrations of D_3 receptors in rat nucleus accumbens and basal ganglia (20 ± 3.6 and 6.6 ± 1.2 fmol/mg of tissue equivalent),[10] we failed to observe a preferential accumulation of [^{11}C]-**1** and [^{11}C]**2** in these regions compared to the cortex or the other regions with lower D_3 receptor density. We only detected a slightly higher uptake in nucleus accumbens 15 min after [^{11}C]**1** injection and 30 min after the [^{11}C]**2** injection. However, these data did not significantly differ from the uptake of the prefrontal cortex and the cerebellum, as confirmed by the tissue-to-plasma ratios reported for [^{11}C]**1** and [^{11}C]**2** in Tables 6 and 7. For both radiotracers, no difference with prefrontal cortex or cerebellum and the remaining part of the basal ganglia was observed.

Autoradiography of [^{11}C]1 and [^{11}C]2 in Rat Brain. To confirm dissection data, [^{11}C]**1** and [^{11}C]**2** distributions were also evaluated ex-vivo on coronal brain sections (one rat for each radiotracer). Radioactivity distribution was evaluated using phosphoimager technique at the time of maximum tracer uptake in the nucleus accumbens, that is, 15 min for [^{11}C]**1** and 60 min for [^{11}C]**2**.

Table 6. Tissue to Plasma Ratio of [^{11}C]**1** in Rats[a]

tissue	5 min	15 min	30 min	60 min
blood	0.79 ± 0.15	0.81 ± 0.03	0.71 ± 0.19	0.84 ± 0.04
prefrontal cortex	0.77 ± 0.02	1.07 ± 0.00	1.11 ± 0.44	1.27 ± 0.10
nucleus accumbens	0.65 ± 0.20	1.41 ± 0.14	1.17 ± 0.25	0.98 ± 0.31
anterior striatum	0.57 ± 0.01	0.89 ± 0.22	0.52 ± 0.73	1.15 ± 0.01
central striatum	0.83 ± 0.10	1.03 ± 0.19	1.02 ± 0.27	1.16 ± 0.09
posterior striatum	0.64 ± 0.06	1.26 ± 0.01	0.93 ± 0.22	1.06 ± 0.15
cerebellum	0.96 ± 0.21	1.14 ± 0.27	1.01 ± 0.37	1.22 ± 0.04

[a] The ratio was calculated as %ID/g of tissue divided per %ID/g of plasma.

For [^{11}C]**2**, no selective retention of the tracer was observed in nucleus accumbens or in striatum with respect to other cerebral areas examined. In agreement with the tissue dissection data, a small [^{11}C]**1** radioactivity accumulation was detected in the nucleus accumbens, but the intensity was comparable with that

Table 7. Tissue to Plasma Ratio of [^{11}C]**2** in Rats[a]

tissue	5 min	15 min	30 min	60 min
blood	0.92 ± 0.11	0.89 ± 0.10	1.01 ± 0.11	1.02 ± 0.25
prefrontal cortex	1.18 ± 0.50	0.94 ± 0.41	2.00 ± 0.21	2.13 ± 0.27
nucleus accumbens	1.01 ± 0.40	0.85 ± 0.33	2.08 ± 0.48	2.26 ± 0.73
anterior striatum	0.93 ± 0.32	0.75 ± 0.23	1.66 ± 0.31	1.61 ± 0.28
central striatum	0.93 ± 0.36	0.86 ± 0.38	1.76 ± 0.30	1.85 ± 0.24
posterior striatum	0.50 ± 0.53	0.75 ± 0.40	1.70 ± 0.48	2.11 ± 0.43
cerebellum	1.04 ± 0.43	0.88 ± 0.39	1.88 ± 0.60	1.61 ± 0.19

[a] The ratio was calculated as %ID/g of tissue divided per %ID/g of plasma.

of prefrontal cortex and only slightly higher than that in the remaining regions.

Discussion

To evaluate the potential application of the new radiotracers [^{11}C]**1** and [^{11}C]**2** for the in vivo PET imaging of D_3 receptors, cerebral distribution and autoradiographic studies in rat were performed. To this aim, the radioactivity concentration (as %ID/g) of these two ligands was determined in cerebral areas in which the presence of D_3 receptors has already been demonstrated by autoradiography and immunoblot experiments[10,11] (Tables 4 and 5). Both [^{11}C]**1** and [^{11}C]**2** are able to cross the blood−brain barrier, and they localize in the brain of animals, but not as expected. In fact, in nucleus accumbens and in basal ganglia, the regions with the highest D_3 receptor concentrations in rat brain,[10] no preferential accumulation of [^{11}C]**1** and [^{11}C]**2** was found. By contrast, Levant and colleagues found in their autoradiogram quantification experiment performed on rat brain with [^{3}H]PD128907[10] a radioactivity concentration ratio of approximately 30 between nucleus accumbens and frontal cortex. In our biodistribution studies nonsignificant differences were registered in [^{11}C]**1** or [^{11}C]**2** uptake between nucleus accumbens and prefrontal cortex (Tables 4 and 5). Both tissue dissection and autoradiographic experiments showed a slight preferential uptake of radioactivity in the nucleus accumbens of rats injected with [^{11}C]**1**, but this accumulation is not specific because of the high uptake also in other brain regions, such as prefrontal cortex, in which the D_3 receptors are present at very low concentration. In rats injected with [^{11}C]**2**, nonspecific uptake was observed in nucleus accumbens or in basal ganglia. This was also confirmed by the data presented in Tables 6 and 7 in which the %ID/g of cerebral areas was divided by the %ID/g of plasma. Nucleus accumbens-to-plasma ratio and basal ganglia-to-plasma ratio did not significantly differ from prefrontal cortex-to-plasma ratio both after [^{11}C]**1** and after [^{11}C]**2** administration. Plasma was considered the reference tissue because of the presence of D_3 receptors in the cerebellum, as shown in immunoblot experiments by Khan and colleagues.[11] The preliminary autoradiographic study confirmed that the biodistribution data for both [^{11}C]**1** and [^{11}C]**2** are in contrast with what was observed by other authors with [^{3}H]PD128907[10] or anti-D_3 receptor specific antibody binding.[11] Our findings are also in contrast with the data of receptor affinity, in which [^{11}C]-**1** and [^{11}C]**2** seemed to have a very high affinity for D_3 compared to the other dopamine receptor subtypes localized also in basal ganglia and to 5-HT_{1A} receptors that are mainly localized in cortex.[12,13] These unexpected results were also obtained by Sovago and colleagues.[7] They used, as a PET putative D_3 receptor ligand, the compound **9** in monkey brain, but despite its promising in vitro binding characteristics, the tracer failed to specifically localize in cerebral D_3-rich areas such as nucleus accumbens. They proposed that the D_3 receptor could be occupied by dopamine in physiological conditions, as demonstrated by Schotte et al.[14] A possible explanation for the small [^{11}C]**1** and [^{11}C]**2** uptake in D_3-rich areas could be the noise represented by the high circulating activity in the blood or the presence of degradation phenomena. In addition, high ClogP[8] values of compounds **1** and **2** may be responsible for their nonspecific accumulation. These assumptions must be verified in the next kinetic work.

In conclusion, the [^{11}C]**1** and [^{11}C]**2** cerebral distribution and the autoradiographic studies performed in rat demonstrated that these new tracers cross the blood−brain barrier and localize in the brain. However, their distribution data in brain did not reflect the real expression of the D_3 receptors, and therefore, [^{11}C]**1** and [^{11}C]**2** are not suitable for in vivo imaging.

Experimental Section

Materials. Column chromatography was performed with 1:30 ICN silica gel 60A (63−200 μm) as the stationary phase. ^{1}H NMR spectra were recorded on a Varian Mercury-VX spectrometer. All chemical shift values are reported in ppm (δ). Recording of mass spectra was done on an Agilent 1100 series LC-MSD trap system UL. Purity of compounds **3** and **4** was checked by HPLC analysis on a Perkin-Elmer series 200 LC instrument using a Phenomenex Prodigy ODS-3 RP-18 column (250 mm × 4.6 mm, 5 μm particle size) and equipped with a Perkin-Elmer 785A UV/VIS detector set at $\lambda = 254$ nm (optimal wavelength for detection of compounds **1**, **2**, **3,** and **4**). All compounds were eluted with CH_3OH/ammonium formiate (25 mM, pH = 3), 9:1 (v/v), at 1 mL/min flow rate.

[^{11}C]Carbon dioxide was produced by the ^{14}N(p,α)^{11}C reaction on a IBA Cyclone 18/9 cyclotron, using an 18 MeV proton beam at currents 15−30 μA, and trapped in a hollow stainless steel loop, cooled with liquid nitrogen. [^{11}C]Methyl iodide was synthesized as described by Crouzel[15] involving the reduction of [^{11}C]CO_2 with $LiAlH_4$ to lithium aluminum−[^{11}C]methylate, hydrolysis of this intermediate organometallic complex, and subsequent iodination of the formed [^{11}C]methanol with hydroiodic acid and distillation through an Ascarite-Sicapent purification column.

Radiochemical syntheses and purifications of the radioligands were performed on the partially modified fully automated synthesis module (PET Tracer Synthesiser, Nuclear Interface Datentechnik GmbH, Münster, Germany) for [^{11}C]-methylation, which has been described in detail elsewhere.[16]

Semipreparative HPLC for radioligands purification was performed using a Sykam pump S1021 connected to an UV detector (model K0021 Knauer) set at 254 nm and to a Geiger Muller radiodetector, with a reversed-phase column (Shandon Hypersil BDS C-18, 5 μm, 250 mm × 10 mm). Elution was carried out at 4 mL/min flow rate with the following mobile-phases: CH_3CN/50 mM sodium dihydrogen orthophosphate-1-hydrate (65:35, v/v) for [^{11}C]**1** and CH_3CN/50 mM sodium dihydrogen orthophosphate-1-hydrate (55:45, v/v) for [^{11}C]**2**.

The final radioligands were analyzed, for their quality control, with a Waters 515 isocratic pump and a Waters 2487 variable-wavelength UV detector set at 254 nm in series with β^+-Bioscan flow count detector, using two different reversed-phase analytical columns: Xterra RP-18 (5 μm, 250 mm × 4.6 mm) and Shandon Hypersil BDS C-18 (5 μm, 250 mm × 4.6 mm) at 1 mL/min flow rate. Data collection for HPLC control was performed by a Waters Millennium 32 chromatography software package.

In the analysis of the ^{11}C-labeled compounds, unlabeled reference standards **1** and **2** were used for comparison in all the HPLC runs. Identity of the final compounds was assessed by mass spectrometry. Authentic standard **1** was dissolved in H_2O/CH_3CN 1:1 (v/v) at a concentration of 1 mg/mL and subsequently diluted 1:100 with H_2O/CH_3CN 1:1 (v/v). An aliquot of the authentic standard **2** and of compounds [^{11}C]**1** and [^{11}C]**2** obtained by the carrier-added radiosyntheses were instead dissolved in CH_3OH. Analyses were performed by APCI/MS as follows. Samples were introduced by a Rheodyne injector with a loop of 10 μL using water/acetonitrile 1:1 (v:v) as delivering solvent at flow rate of 200 μL/min generated with a Agilent 1100 HPLC system (Agilent Technologies Inc. Palo Alto, CA) directly into the APCI source of the mass spectrometer. The APCI spectra were recorded with a Esquire 3000 Plus Ion Trap Mass Spectrometer (Bruker Daltonics GmbH Bremen Germany). The corona discharge was set at 4000 nA, nebulizer at 25 psi, dry gas at 5 L/min, dry temperature at 180 °C, APCI temperature at 300 °C, and capillary voltage at 4 KV working with the following smart parameter settings: target mass was set at *m/z* 486 and 476 for **1** and for **2**, respectively; compound stability was set to 100% and trap drive level to 100%, and the normal optimization feature was used. Spectra were recorded by scanning from *m/z* 50 to 1000 working with an ICC target of 15 000.

The pH of the final solutions was measured on a Schott Geräte pH-meter. Pyrogenity tests were performed using the Limulus Amebocyte Lysate (LAL) test (Bio Whittaker, Inc.).

***N*-[4-[4-(2,3-Dichlorophenyl)piperazin-1-yl]butyl]-1-hydroxy-2-naphthalenecarboxamide (3).** A solution of **1** (0.61 g, 1.26 mmol) in anhydrous DMF was dropped under N_2 to a mixture of sodium thioethoxide (0.27 g, 3.2 mmol) in the same solvent (10 mL). The reaction mixture was heated at 100 °C, under stirring, for 9 h. The solvent was then evaporated under reduced pressure, and the residue was taken up with EtOAC and washed several times with H_2O. The organic layer was dried over anhydrous Na_2SO_4 and concentrated in a vacuum. The crude residue was chromatographed on a silica gel column using $CHCl_3/CH_3OH$, 19:1 v/v, as eluent to give **3** as a white semisolid (0.3 g, 51% yield) with over 99% purity as determined by HPLC. ^{1}H NMR (300 MHz, acetone-d_6): δ 1.68−1.78 [m, 4H, $NHCH_2(CH_2)_2$], 2.54 [t, 2H, J = 6.5 Hz, $CH_2N(CH_2)_2$], 2.69 [br s, 4H, $CH_2N(CH_2)_2$], 3.09 [br s, 6H, $(CH_2)_2NAr$, NH, OH, 1H D_2O exchanged], 3.54 (t, 2H, J = 6.5 Hz, $NHCH_2$), 7.10−8.37 (m, 9H, aromatic). ESI/MS: mass spectrum displayed intense ion at *m/z* 472 corresponding to the protonated molecular ion (M^+) of compound **3** .

***N*-[4-[4-(2,3-Dichlorophenyl)piperazin-1-yl]butyl]-7-hydroxy-2-benzofurancarboxamide (4).** Following the above procedure, we obtained the title compound from **2** in 60% yield. The purity of **4** was over 99% as determined by HPLC. ^{1}H NMR (300 MHz, DMSO-d_6): δ 1.53 [br s, 4H, $NHCH_2(CH_2)_2$], 2.61 [br s, 2H, $CH_2N(CH_2)_2$], 2.78 [br s, 4H, $CH_2N(CH_2)_2$], 3.01 [br s, 4H, $(CH_2)_2NAr$], 3.28 (br s, 2H, $NHCH_2$), 6.83−7.44 (m, 7H, aromatic), 8.62 (br t, 1H, NH), 13.51 (s, 1H, OH, D_2O exchanged). ESI/MS: mass spectra displayed intense ions at *m/z* 464 corresponding to the protonated molecular ion (M^+ + 2) and *m/z* 462 corresponding to the protonated molecular ion (M^+) of compound **4**.

No-Carrier-Added Radiosynthesis of *N*-4[4-[(2,3-dichlorophenyl)piperazin-1-yl]butyl]1-([^{11}C]methoxy)-2-naphthalencarboxamide ([^{11}C]1). [^{11}C]Methyl iodide was transported by a stream of argon into the reaction vessel at 80 °C containing **3** (1.0 mg, 0.002 mmol), anhydrous HMPA (100 μL, dried over 5 Å molecular sieves), and *tert*-BuOK (1.4 mg, 0.012 mmol). After [^{11}C]methyl iodide transfer, the reaction mixture was heated for 5 min at 100 °C, then cooled at room temperature, diluted with a 1:1 (v/v) mixture of CH_3CN/H_2O (1 mL), and injected onto a HPLC semipreparative column. The fraction corresponding to [^{11}C]**1** was eluted at 12−14 min and collected in 30 mL of sterile water acidified with 6 N HCl (1 mL). The product was recovered by solid-phase extraction (SPE) on a Sep-Pak tC-18 plus cartridge (Waters) preactivated with 5 mL of EtOH, followed by 20 mL of water. The Sep-Pak was washed with water (10 mL) before elution with EtOH (0.5 mL) and sterile saline solution (9.5 mL). The final solution was sterilized through a Gelman Acrodisc 0.22 μm sterile filter. The pH of the solution ranged from 6.5 to 7.

The UV and radio-HPLC quality control was carried out on an XTerra reverse-phase column eluted with CH_3CN/50 mM sodium dihydrogen orthophosphate-1-hydrate (60:40, v/v). The amount of carrier was calculated from the UV absorbance peak by means of the external standard calibration plot. The minimal detectable concentration of **1** was 1.84 nmol/mL.

No-Carrier-Added Radiosynthesis of *N*-[4-[4-(2,3-dichlorophenyl)piperazin-1-yl]butyl]-7-([^{11}C]methoxy)-2-benzofurancarboxamide ([^{11}C]2). [^{11}C]Methyl iodide was transported by a stream of argon into the reaction vessel at 80 °C containing **4** (1.0 mg, 0.002 mmol), DMSO (100 μL), and 5 M KOH (2 μL, 0.010 mmol). After 5 min, the reaction mixture was cooled at room temperature, diluted with 1 mL of mobile phase, and injected onto a HPLC semipreparative column. The fraction corresponding to [^{11}C]**2** was eluted at 12−14 min and collected in 30 mL of sterile water acidified with 6 N HCl (1 mL). The product was recovered by solid-phase extraction (SPE) on a Sep-Pak tC-18 plus cartridge (Waters) preactivated with 5 mL of EtOH, followed by 20 mL of water. The Sep-Pak was washed with water (10 mL), before elution with ethanol (0.5 mL) and sterile saline solution (9.5 mL). The final solution was sterilized through a Gelman Acrodisc 0.22 μm sterile filter. The pH of the solution ranged from 6.5 to 7.

The UV and radio-HPLC quality control was carried out on an analytical reversed-phase column X-Terra RP18 eluted with CH_3CN/50 mM sodium dihydrogen orthophosphate-1-hydrate (50:50, v/v). The amount of carrier was calculated from the UV absorbance peak by means of the external standard calibration plot. The minimal detectable concentration of **2** was 1.96 nmol/mL.

Carried-Added Radiosyntheses of [^{11}C]1 and [^{11}C]2. The syntheses were carried out as described above for the no-carried-added preparations, but 20 μL of methanol carrier was added to the hydroiodic acid used for [^{11}C]methyl iodide formation. After semipreparative HPLC purification, the fraction corresponding to the desired radioligand was collected in 30 mL of sterile water acidified with 6 N HCl (1 mL), and the product was recovered by SPE on a Sep-Pak tC18 plus cartridge (Waters) by elution with 1 mL of EtOH. The nonradioactive material with the ^{11}C-labeled radioligands was ensured by the well-detectable UV peak at the retention time of the target compound. The peak was collected and its identity was confirmed by mass spectrometry.

[^{11}C]1. Mass spectrum of pure **1** displayed an intense ion at *m/z* 486 corresponding to the protonated molecular ion (MH^+). The intense ion at +2 Da of the molecular weight of **1** (*m/z* 488) is due to the presence of chlorine atoms in the chemical structure of the analyzed compound. The isotopic distribution evaluated by APCI/MS well corresponds to that calculated by means of IsoPro software (version 3.0). An identical spectrum was obtained when the [^{11}C]**1** obtained by carried-added radiosynthesis was analyzed.

[^{11}C]2. Identity of the [^{11}C]**2** obtained by carried-added radiosynthesis was ensured by comparison of its mass spectrum with that of the pure compound. Mass spectrum of pure **2** displayed an intense ion at *m/z* 476 corresponding to the protonated molecular ion (MH^+). The other intense ion at +2 Da of the molecular weight of **2** (*m/z* 478) is due to the presence of chlorine atoms in chemical structure of the analyzed compound. The isotopic distribution evaluated by APCI/MS well corresponds to that calculated by means of IsoPro software (version 3.0). An identical spectrum was obtained when the [^{11}C]**2** obtained by carried-added radiosynthesis was analyzed.

Addition of authentic standards **1** and **2** to the preparations before HPLC analyses caused the expected increase of the UV peak coeluting with the radioactive materials. Analyses were carried out using two different chromatographic conditions as follows:

[^{11}C]1. (a) Column Hypersil BDS C18; mobile phase CH_3CN/10 mM sodium dihydrogen orthophosphate-1-hydrate 80:

20 (v/v); R_t(**1**) = 7 min; R_t(**3**) = 7.7 min. (b) Column XTerra RP18; mobile phase CH_3CN/50 mM sodium dihydrogen orthophosphate-1-hydrate 60:40 (v/v); R_t(**1**) = 4.5 min; R_t(**3**) = 5.8 min.

[^{11}C]2. (a) Column Hypersil BDS C18; mobile phase CH_3-CN/25 mM sodium dihydrogen orthophosphate-1-hydrate 70:30 (v/v), pH 7.2; R_t(**2**) = 6.2 min; R_t(**4**) = 4.3 min. (b) Column XTerra RP18; mobile phase CH_3CN/ 50 mM sodium dihydrogen orthophosphate-1-hydrate 50:50 (v/v); R_t(**2**) = 5.6 min; R_t-(**4**) = 4.5 min.

Tissue Distribution Studies. Rodent Experiments with [^{11}C]1 and [^{11}C]2. Animals. Rat experiments were performed on albino male rats weighing 225−250 g (Charles River, Italy). Animal experiments were approved by the Ethical Committee for animal care of the San Raffaele Hospital (IACUC) and carried out in accordance with the Italian and EEC recommendations for the care and use of laboratory animals.

Kinetic Experiments. [^{11}C]2 Distribution. The radiotracer [^{11}C]**2** was diluted to a final volume of 100 μL in saline solution and injected in a rat tail vein using a 0.5 mm × 9.5 mm syringe needle. The distribution of [^{11}C]**2** was assayed at 5, 15, 30, 60, and 90 min (n = 3 at each time point) after the injection of approximately 5.3 ± 0.5 MBq of [^{11}C]**2** corresponding to 130 ± 20 pmol of cold compound. Under a light anaesthesia, animals were killed by decapitation at the above times, and the blood samples were collected into heparinized tubes, a part of which was counted in a gamma counter, and the remaining part was centrifuged for the plasma radioactivity determination. The brain was rapidly removed from the skull and discrete cerebral areas (hippocampus, hypophysis, hypothalamus, striatum, cerebellum, cortex) were dissected out and placed in preweighed tubes. Peripheral organs such as heart, lung, stomach, adrenal gland, kidney, spleen, testis, colon, and muscle were also dissected out and placed in preweighed tubes. The radioactivity was counted in a gamma counter and the radioactivity concentration calculated as the percentage of injected dose per gram of tissue (%ID/g).

[^{11}C]1 and [^{11}C]2 Cerebral Distribution. The two radiotracers, [^{11}C]**1** and [^{11}C]**2**, were diluted to a final volume of 100 and 200 μL, respectively, in saline solution and separately injected in a rat tail vein using a 0.5 mm × 9.5 mm syringe needle. The cerebral distribution of [^{11}C]**1** and [^{11}C]**2** was assayed at 5, 15, 30, and 60 min (n = 3 at each time point) after the injection of approximately 6.5 ± 0.5 MBq of [^{11}C]**2** (corresponding to 481 ± 102 pmol of cold compound) and 3.1 ± 0.6 MBq of [^{11}C]**1** (corresponding to 229 ± 22 pmol of cold compound). At the above times, the animals were sacrificed by decapitation under light ether anaesthesia, and a blood sample was collected into heparinized tubes, a part of which was counted in a gamma counter, and the remaining part was centrifuged for the plasma radioactivity determination. The brain was rapidly removed from the skull and correctly positioned in a specific rat brain matrix (Stoleting, Chicago, IL). Coronal sections of 2 mm thickness were sequentially performed starting from the prefrontal cortex. Every section was placed on the plane, and according with the morphological coordinates of stereotaxic atlas,[17] discrete cerebral areas (frontal cortex, nucleus accumbens, anterior striatum, medial striatum, posterior striatum, and cerebellum) were dissected out and placed in preweighed tubes. The radioactivity was counted in a gamma counter, and the concentration was calculated as the percentage of injected dose per gram of tissue (%ID/g).

[^{11}C]1 and [^{11}C]2 Autoradiography. The two radiotracers, [^{11}C]**1** and [^{11}C]**2**, were diluted to a final volume of 200 μL in saline solution and separately injected in the rat tail vein using a 0.5 mm × 9.5 mm syringe needle (one animal for each tracer). Images of radioactivity distribution were obtained at 60 min after the injection of 9.1 MBq of [^{11}C]**2** (corresponding to 793 pmol of cold compound) and 15 min after the injection of 2.7 MBq of [^{11}C]**1** (corresponding to 241 pmol of cold compound) using a phosphorimaging technique. In practice, the animals were sacrificed by decapitation (under ether anaesthesia) at the indicated times, and then the brain was rapidly removed from the skull and correctly positioned in a specific rat brain matrix (Stoelting). Coronal sections of 2 mm thickness were sequentially performed starting from the prefrontal cortex, transferred on a film, and exposed at the multipurpose storage screen for 100 min in a dark room, and then acquired for 10 min with a Cyclone storage phosphor system (Camberra Packard).

References

(1) Levant, B. The D_3 Dopamine Receptor: Neurobiology and Potential Clinical Relevance. *Pharmacol. Rev.* **1998**, *49*, 231−252.

(2) Jaber, M.; Robinson, S. W.; Missale, C.; Caron, M. G. Dopamine Receptors and Brain Function. *Neuropharmacology* **1997**, *35*, 1503−1519.

(3) Ehrin, E.; Farde, L.; de Paulis, T.; Eriksson, L.; Greitz, T.; Johnstrom, P.; Litton, J. E.; Nilsson, J. L.; Sedvall, G.; Stone-Elander, S.; Ögren, S. Preparation of ^{11}C-Labeled Raclopride, a New Potent Dopamine Receptor Antagonist: Preliminary PET Studies of Cerebral Dopamine Receptors in the Monkey. *Int. J. Appl. Radiat. Isot.* **1985**, *36*, 269−273.

(4) Mukherjee, J.; Christian, B. T.; Dunigan, K. A.; Shi, B.; Narayanan, T. K.; Satter, M.; Mantil, J. Brain Imaging of ^{18}F−Fallypride in Normal Volunteers: Blood Analysis, Distribution, Test-Retest Studies, and Preliminary Assessment of Sensitivity to Aging Effects on Dopamine D_2/D_3 Receptors. *Synapse* **2002**, *46*, 170−188.

(5) de Vries, E. F. J.; Elsinga, P. H.; van Waarde, A.; Kortekaas, R.; Dijkstra, D.; Vaalburg, W. Synthesis of the Dopamine D_3 Receptor Antagonist [^{11}C]GR218231. *J. Labelled Compd. Radiopharm.* **2003**, *46*, S140.

(6) Tu, Z.; Huang, Y.; Vangveravong, S.; Blair, j. B.; Luedtke, R. R.; Dence, C.; Mach, R. H. Conformationally-Flexible Benzamide Analogues as Dopamine D_3 Receptor Imaging Agents for PET and SPECT. *J. Labelled Compd. Radiopharm.* **2003**, *46*, S170.

(7) Sovago, J.; Farde, L.; Halldin, C.; Langer, O.; Laszlovszky, I.; Kiss, B.; Gulyas, B. Positron Emission Tomographic Evaluation of the Putative Dopamine-D_3 Receptor Ligand, [^{11}C]RGH-1756 in the Monkey Brain. *Neurochem. Int.* **2004**, *45*, 609−617.

(8) Leopoldo, M.; Berardi, F.; Colabufo, N. A.; De Giorgio, P.; Lacivita, E.; Perrone, R.; Tortorella, V. Structure-Affinity Relationship Study on N-[4-(4-arylpiperazin-1- yl)butyl]arylcarboxamides as Potent and Selective Dopamine D_3 Receptor Ligands. *J. Med. Chem.* **2002**, *45*, 5727−5735.

(9) Feutrill, G. I.; Mirrington, R. N. Demethylation of Aryl Ethers with Thioethoxide Ion in Dimethyl formamide. *Tetrahedron Lett.* **1970**, *16*, 1327−1328.

(10) Levant, B. Differential Distribution of D_3 Dopamine Receptors in the Brains of Several Mammalian Species. *Brain Res.* **1998**, *800*, 269−274.

(11) Khan, Z. U.; Gutierrez, A.; Martin, R.; Penafiel, A.; Rivera, A.; De La Calle, A. Differential Regional and Cellular Distribution of Dopamine D_2−Like Receptors: an Immunocytochemical Study of Subtype-Specific Antibodies in Rat and Human Brain. *J. Comp. Neurol.* **1998**, *402*, 353−371.

(12) Meador-Woodruff, J. H. U. Update on Dopamine Receptors. *Ann. Clin. Psychiatry* **1994**, *6*, 79−90.

(13) Barnes, N. M.; Sharp, T. A Review of Central 5-HT Receptors and Their Function. *Neuropharmacology* **1999**, *38*, 1038−1152.

(14) Schotte, A.; Janssen, P. F.; Bonaventure, P.; Leysen, J. E. Endogenous Dopamine Limits the Binding of Antipsychotic Drugs to D_3 Receptors in the Rat Brain: a Quantitative Autoradiographic Study. *Histochem. J.* **1996**, *28*, 791−799.

(15) Crouzel, C.; Långström, B.; Pike, V. W.; Coenen, H. H. Reccomendations for a Practical Production of [^{11}C]Methyl Iodide. *Appl. Radiat. Isot.* **1987**, *38*, 601−603.

(16) Matarrese, M.; Soloviev, D.; Todde, S.; Neutro, F.; Petta, P.; Carpinelli, A.; Brüssermann, M.; Galli Kienle, M.; Fazio, F. Preparation Of [^{11}C]Radioligands With High Specific Radioactivity On a Commercial PET Tracer Synthesizer. *Nucl. Med. Biol.* **2003**, *30*, 79−83.

(17) Paxinos, G.; Watson, C. *The Rat Brain in Stereotaxic Coordinates*; Academic Press: San Diego, CA, 1998.

JM050171K